

SUPPRESSION EFFECT OF NICKEL FOAM ON THE EXPLOSION OF METHANE/ETHANE MIXTURE

Dongping YANG^{1*}, Yulong DUAN^{2,3**}, Min GUO¹, Weibin WANG¹, Yang LIU¹

1. SINOPEC Shengli Oilfield Technical Testing Center, Dongying, 257000, China;

2. College of Safety Engineering, Chongqing University of Science and Technology, Chongqing, 401331, China

3. Chongqing Key Laboratory for Oil and Gas Production Safety and Risk Control Technology, Chongqing, 401331, China

Methane and ethane are the main components of natural gas and coal bed gas in some regions of China, and the presence of ethane further exacerbates the risk of explosions, posing significant safety challenges during the production, storage, transportation, and use of natural gas. This study utilizes a self-constructed small-size experimental platform to investigate the suppression effect of nickel foam on the explosion of methane/ethane mixture in explosion tubes. The results show that nickel foam has two different effects on the methane/ethane flame: promotion and suppression. When the explosion flame quenching fails, the explosion is more violent, the flame propagation velocity and the peak explosion overpressure are both increased, and the peak velocity, the peak pressure, appear at the second wave; when the explosion flame quenching successfully, the flame propagation velocity peak and the explosion overpressure peak are attenuated, and the velocity peak and pressure peak appear in the first wave. 40PPI nickel foam has the best effect on methane/ethane mixture explosion suppression.

Keywords: Methane/ethane; Nickel foam; Explosive characteristics; Suppression

1 Introduction

With the development of the economy and the adjustment of the global energy structure, gas fuel has become increasingly widely used for its high heat energy, low pollution, and low cost [1]. Natural gas consists mainly of methane, ethane, and other small amounts of alkanes [2]. And also, Coal bed gas in some areas appears as “wet gas” with 5% to 43% heavy hydrocarbon content, of which the ethane component accounts for more than 90% of the total heavy hydrocarbon gas [3]. The presence of ethane can increase the risk of explosions, causing significant safety challenges during the production, storage, transportation, and use of natural gas.

Methane and ethane as the major components of natural gas, associated oilfield gas, and “wet coal bed gas”. The uncertainty of explosion hazards caused by methane/ethane mixture attracts many scholars to study it. Su et al. [4] investigated the relationship between flame emission spectra and explosion characteristics of methane/ethane/air mixtures, They found that in the fuel-poor state, P_{\max} and $(dP/dt)_{\max}$ increase with ethane, while the time to reach P_{\max} decreases with ethane. It has been confirmed that the more hydrocarbons such as ethane account for in the natural gas composition, the flame propagation speed, peak explosion pressure, and maximum rate of pressure rise increase gradually [4]. Therefore, research on explosion isolation and suppression technologies to reduce the explosion hazards of methane/ethane mixtures is very important to ensure the safe production and transportation of explosive gas.

The main suppression methods of gas explosion are porous media [6], inert gases [7], fine water mists [8], and solid powders [9]. Among them, porous materials are widely used in explosion suppression [10] because of their unique pore structure and environmental protection, high hardness, high-temperature resistance, strong resistance to sintering, and other advantages [11]. Currently, studies on the effect of porous materials on gas explosion suppression mainly focus on the research areas of methane and methane/hydrogen mixtures. However, little research has been done

* Corresponding author, e-mail: Dongping YANG (3894857371@qq.com)

** Corresponding author, e-mail: Yulong DUAN (14924928@qq.com)

on suppressing methane/ethane mixture explosions by porous materials. Therefore, it is essential to study the influence of porous materials on the explosive characteristics of methane/ethane gas and to reveal their intrinsic mechanisms that promote or inhibit the explosive behavior of methane/ethane gas.

The unique pore structure of porous materials can effectively inhibit explosion overpressure and quench the flame [12]. When the explosion shock wave and explosion flame pass through the porous material, the pressure wave will be reflected at different angles due to the porous material's structure [12], the collision chances of the active radicals in the explosion and combustion reactions with the inner wall of the porous pores increase dramatically, and many free radicals lose their activity. Thus achieving the purpose of reducing the peak explosion overpressure and flame temperature and accelerating the flame quenching. If quenching fails, the porous material acts as an obstacle to accelerate flame propagation [15], resulting in more serious consequences. Long et al. [16] found that 20 PPI porous material fails to quench a low hydrogen methane explosion flame and escalated the explosion. However, 40 PPI porous material can quench the flame successfully. Wu [17] shows that 10 PPI porous material promotes the explosion flame, and 30 PPI porous material is very easy to promote the flame to form a localized explosion due to the large blocking ratio, resulting in failure suppression. Other studies have shown that the failure of explosion suppression in porous materials may also depend on the properties of the combustible gas itself. Zhou et al. [18] found that mesh aluminum alloy and aluminum velvet can suppress methane/air mixture gas explosions, but promote hydrogen/air and acetylene/air mixture gas explosions in their experiments.

In conclusion, most of the current research has focused on investigating the suppression effect of porous materials on single gas or analyzing the explosion characteristics of methane/ethane gas mixtures only. However, little research has been done on the effect of porous materials on the explosion suppression of methane/ethane mixtures. In this paper, widely used porous materials with different porosities of 30PPI and 40PPI was selected to study the explosion characteristics of a methane/ethane mixture with ethane volume fractions of 10%, 20%, and 30%, respectively, and explore the suppression effect of porous materials on the methane/ethane explosion. The relevant research results can provide data support and theoretical basis for the explosion prevention and suppression of natural gas and its associated gas, petroleum gas, coalbed methane, etc. during extraction and transportation.

2 Experimental setup

2.1 Experimental platform construction

As shown in [Fig. 1](#), the experimental platform used in this study mainly consists of an experimental bench, an explosion experimental pipe, a gas distribution system, an ignition system, a flame image acquisition system, and a pressure acquisition system. The explosion experiment pipeline consists of 100 mm × 100 mm × 1000 mm square pipe and porous foam nickel composition; the square pipe can withstand the internal pressure of 2MPa, and the pipe wall thickness is 20mm. Both ends of the pipe are closed with a thickness of 10mm steel plate with silicone pads; the left side of the steel plate is reserved for ventilation and ignition head installation port, and the right side of the steel plate is reserved for the exhaust port, in the pipeline at the top of the tail to take the diameter of 3cm of the explosion relief port. In all experiments, the vents were covered and sealed with PVC film. The gas distribution system consisted of methane gas cylinders, ethane gas cylinders, air gas cylinders, and three mass flow meters. Methane and ethane were 99.99% pure, ambient air was used for the air, and the mass flow meter was a high sensitivity mass flow control meter from Alicat (range 0~5 L/min, meter error ±0.4% of reading). The experiments were carried out at an equivalence ratio of 1.0 and a mixture of 10% ~ 30% ethane. Calculate the gas flow ratio parameters from equations (1) and (2).

$$\varphi = n_{fuel} / n_{air} / (n_{fuel} / n_{air})_{stopc} \quad (1)$$

$$\varphi = n_{C_2H_6} / (n_{C_2H_6} / n_{CH_4}) \times 100\% \quad (2)$$

A 4-fold volume gas distribution method was used to ensure that the remaining gas in the pipeline was discharged [19]. By calculating the volume of the relevant pipeline and reading the flow meter, we estimate that the time required to fill the pipeline at ambient temperature and pressure entirely is approximately 2 minutes. In addition, the exhaust system located on the right side of the pipeline can effectively exhaust all gases in the exhaust pipeline, thereby promoting the air replacement process

inside the pipeline, which involves using a mixture of air and fuel to replace the original air in the pipeline. This inflation phase is expected to last for 8 minutes.

The ignition system comprises a homemade ignition head, a high-frequency pulse igniter, an ignition controller, and an ignition power supply (4 batteries). The power supply input voltage is 6V. Two platinum wires with a diameter of 0.1 mm are welded at the ignition position to produce a high-temperature spark. The flame image acquisition system comprises a PhantomV710L high-speed camera and PCC graphics processing software. The camera is set at 1280×240 pixels and shoots at 2000fps. The pressure acquisition system comprises two pressure sensors and a data acquisition module. Pressure sensor 1 (from now on referred to as "P1") is installed at a distance of 17.5 cm from the ignition head, and pressure sensor 2 (from now on referred to as "P2") is installed at a distance of 77.5 cm from the ignition head, pressure sensors pick up signals of pressure changes at both ends of the porous material. The pressure sensor has a range of 0 ~ 690 kPa and a linearity error of less than 1%.

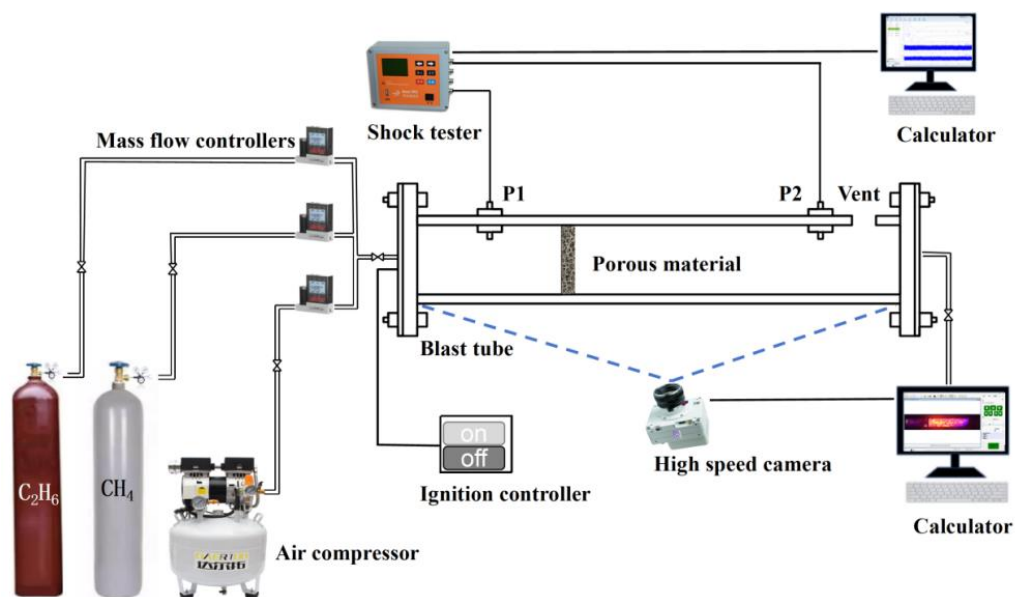


Fig. 1 Diagram of the experimental setup

2.2 Experimental methods and working conditions

As shown in Fig. 2, two types of nickel foam with different porosity were selected for the porous material, and the pore density unit PPI (Pores Per Linear Inch) was 30 and 40, respectively. The nickel foam cross-section size is 100 x 100 mm² with a thickness of 10 mm, and the nickel foam is mounted in a fixed position (300 mm from the ignition end). To ensure the accuracy of the experiments, each of the nine sets of experimental conditions shown in Tab. 1 was repeated 3-4 times.

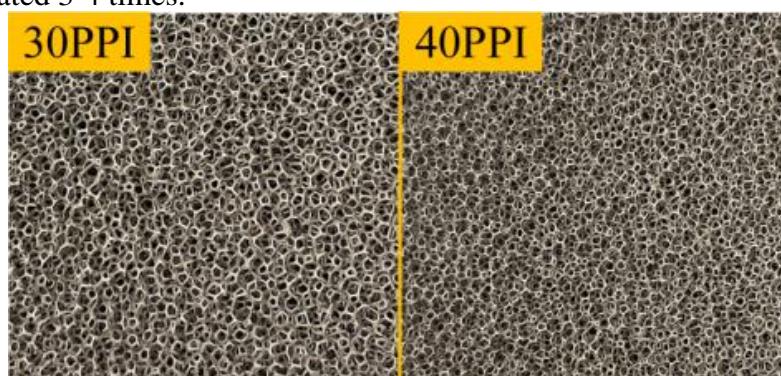


Fig. 2 Porous material-nickel foam

Tab. 1 Experimental conditions

Serial number	Ethane volume fraction ϕ /%	Porosity of porous materials (PPI)
C1	10	-
C2	20	-
C3	30	-
C4	10	30
C5	20	30
C6	30	30
C7	10	40
C8	20	40
C9	30	40

3 Analysis of experimental results

3.1 Flame structure changes

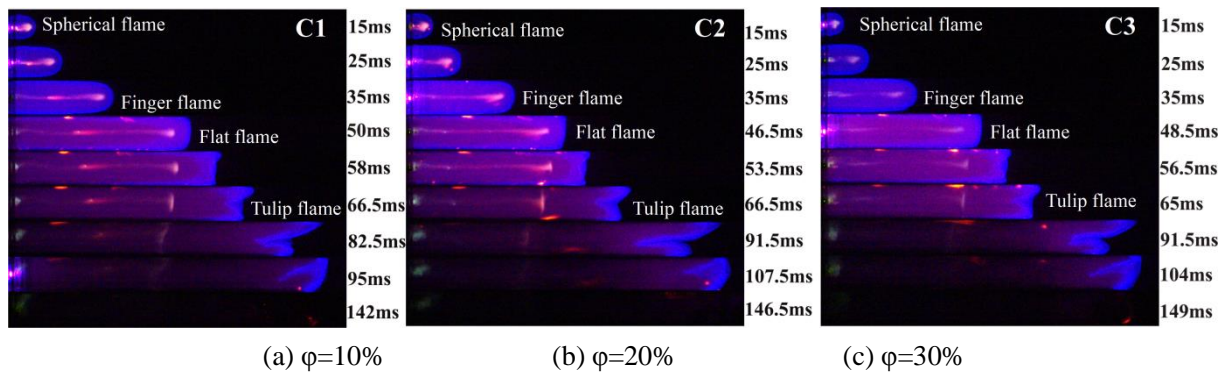


Fig. 3 Dynamic flame propagation process of methane/ethane mixture explosion in an empty pipe

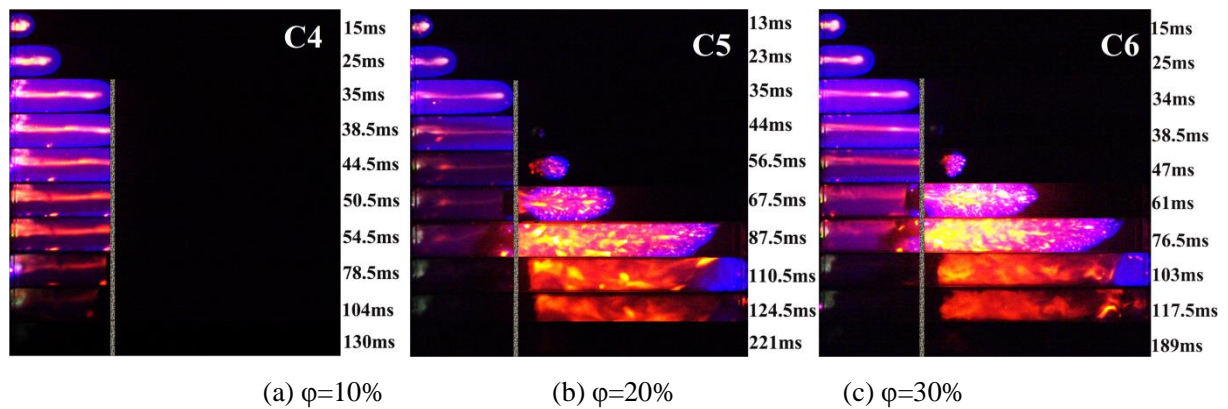


Fig. 4 Effect of nickel foam (30PPI) on flame propagation in methane/ethane mixture explosion

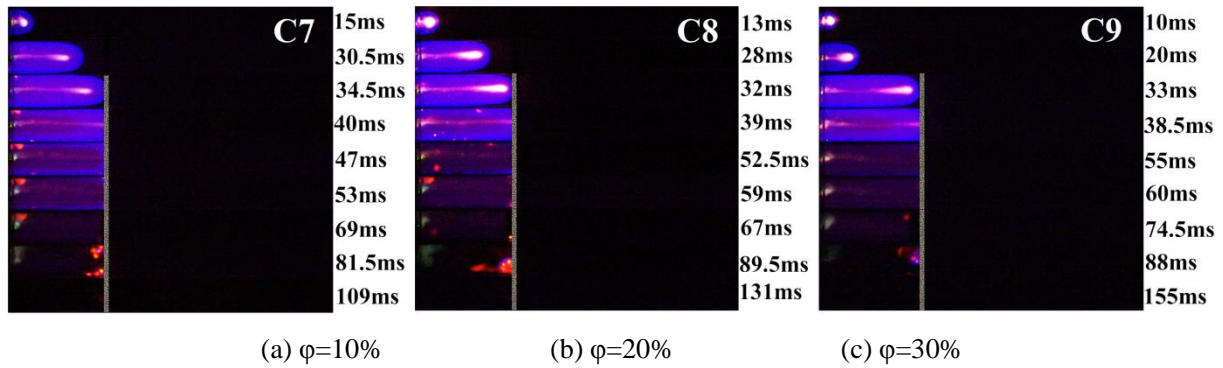


Fig. 5 Effect of nickel foam (40PPI) on flame propagation in methane/ethane mixture explosion

Hu et al. [21] found in 1996 that the combustion propagation process of combustible gases in pipelines can be divided into four stages, i.e., the spherical flame stage, the finger flame stage, the flat flame stage, and the "tulip" flame stage. Fig. 3 shows the dynamic propagation process of the methane/ethane mixture explosion flame in an empty pipe. As shown in Fig. 3, the flame propagation process in all three concentrations is from spherical to finger to plane to "tulip" shape, and finally, the flame is transmitted to the end of the pipe, and the combustion reaction is completed and extinguished. For example, in Fig. 3(a), when the ethane volume fraction $\phi=10\%$, the structural change of the methane/ethane mixture explosion flame front went through four stages: spherical flame ($t=15\text{ms}$), finger flame ($t=35\text{ms}$), plane flame ($t=50\text{ms}$) and tulip flame ($t=66.5\text{ms}$).

Comparison of Fig. 3 (a), (b), and (c) can be seen. The empty pipe selected ethane volume fractions of 10%, 20%, and 30%, respectively, to carry out experimental studies on the methane/ethane mixture of the evolution of the flame front structure of the explosion does not have a significant difference, have gone through the above four stages. With increasing volume fraction of ethane, the explosion process of premixed gases is more rapid and violent [22]. As shown in Fig. 3(b) at 46.50 ms and Fig. 3(c) at 48.5 ms, the planar-shaped structure of Fig. 3(b), (c) reaches faster compared to that of Fig. 3(a) at 50 ms.

When there is porous material in the explosion experiment pipeline, the propagation process of premixed methane/ethane gas explosion flame is effected by porous material with different porosity, the flame structure between the conditions appears apparent differences, and with the increase of ethane proportion in the premixed gas, the degree of flame variation becomes greater [4].

Fig. 4 shows the effect of nickel foam with a porosity of 30 PPI on the dynamic flame propagation process of methane/ethane mixture explosion. Fig. 4(a) shows that the flame failed to penetrate the porous material when the volume fraction of ethane is 10%, and the porosity of the porous material is 30 PPI. However, in Fig. 4(b) and (c), increasing the proportion of ethane in the premixed methane/ethane gas, the premixed combustion reaction becomes more intense, the porous material fails to block the flame, flame penetrates the porous materials, as shown in Fig. 4(b) at $t = 67.5\text{ms}$ and Fig. 4(c) at $t = 61\text{ms}$. The flame passes through the porous material and ignites the downstream explosive mixture gas, and the flame rapidly fills the pipe, spreading irregularly from left to right. The center of the flame shows a chaotic and disorderly state, and the color is bright yellow. Flame front laminar flow combustion is destroyed, turbulence is increased, and the color is light blue. The whole process of propagation no longer appears as a "tulip" flame structure. Accelerated propagation above the flame front toward the vent. When the solid phase structure of foam nickel cannot extinguish the flame through its energy absorption, it may cause secondary deflagration. This is because the flame will be split into many small jet flames when passing through the porous microchannels, and the limited energy absorption capacity of foam nickel has a limited effect on these small flames. These small flames propagate downstream along the porous material, igniting the unburned gas and leading to detonation. In this process, porous materials can be seen as a mesh-like obstacle, which not only blocks the propagation path of some flames but also promotes the transition from laminar flames to turbulent flames, thereby intensifying the intensity of the explosion.

Fig. 5 shows the effect of nickel foam with a porosity of 40 PPI on the dynamic flame propagation process of a methane/ethane mixture explosion. Fig. 5 is different from Fig. 4 in that when the nickel foam porosity is 40 PPI, the increase in porosity further increases the number of tiny channels inside the nickel foam. Thus, flame propagation is blocked and quenched, and the flame fails to penetrate the porous material. As can be seen from Fig. 5, after the premixed gas is ignited and

propagates along the pipe to the pressure relief port, the flame structure evolves from hemispherical to finger-shaped, and in the transition from finger-shaped to plane-shaped, the flame front contacts the nickel foam and then enters into the interior of the nickel foam. Because of the existence of a certain number of disordered pore structures within the nickel foam, at this time, the flame edge contacts the pipeline wall, and the flame front is in the deceleration stage. Therefore, the flame energy entering the porous interior is gradually converted and absorbed, and the flame is cooled and quenched.

Comparison of Fig. 4 and Fig. 5 can be found when the nickel foam porosity of 30 PPI, the explosion flame propagation appeared to produce quenching success or quenching failure of the two effects, when the volume fraction of ethane is 10%, nickel foam successfully quenched the flame, while the volume fraction of ethane is 20% and 30%, quenching failure occurs, and the flame intensifies, resulting in a secondary explosion phenomenon. The explosion flame is successfully quenched when the nickel foam porosity is 40 PPI.

3.2 Flame front velocity

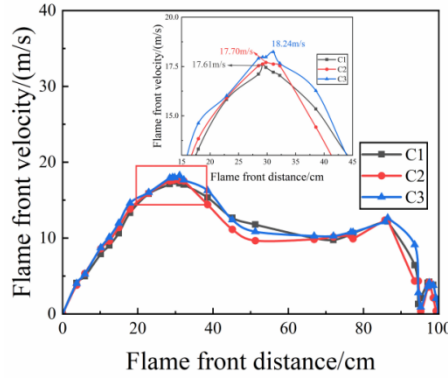


Fig. 6 Flame propagation velocity of methane/ethane mixture explosion in an empty pipe

The flame front velocity in the pipe depends on the flame propagation distance and the corresponding time interval Δt . The flame propagation distance is determined by the position of the leading edge of the flame front (L_1 , L_2) corresponding to the two-time points (t_1 , t_2). Flame velocity equation is shown in (3).

$$v = \frac{\Delta L}{\Delta t} = \frac{L_2 - L_1}{t_2 - t_1} \quad (3)$$

Fig. 6 shows the flame propagation velocity of methane/ethane mixture explosion in an empty pipeline. It can be seen that the overall trend of the explosion flame propagation velocity in the pipeline increases first and then decreases, reaches the peak at about 30cm from the ignition source.. The peak flame velocity is 17.61 m/s when $\phi = 10\%$, 17.70 m/s when $\phi = 20\%$, and 18.24 m/s when $\phi = 30\%$. As can be seen from Fig. 6, the empty pipe selected different volume fractions of ethane to carry out experimental studies; the methane/ethane mixture explosion flame propagation velocity trend is not significantly different, and, with the increase of the volume fraction of ethane increases, the explosion reaction of methane/ethane mixture increases, and the flame propagation speed accelerates.

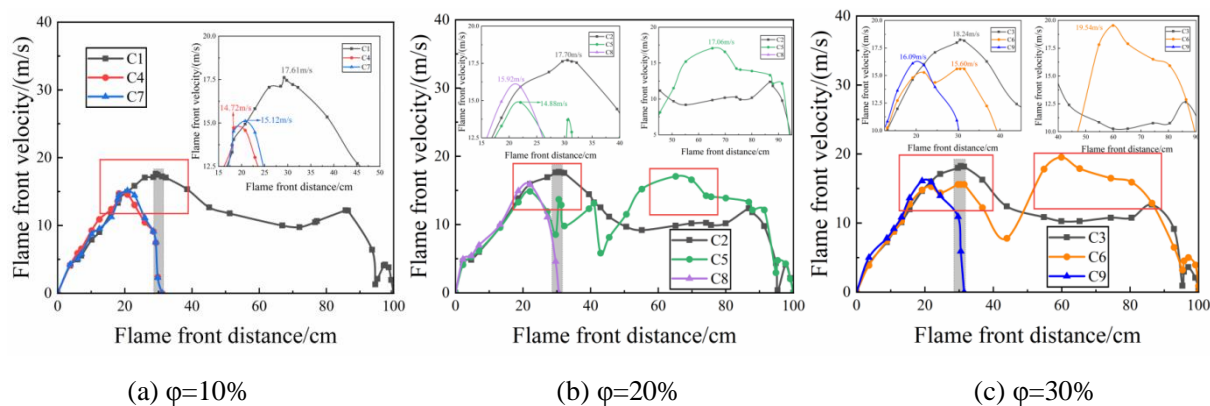


Fig. 7 Explosion flame velocity versus flame front distance for different porosity of nickel foam

Fig. 7 shows the relationship between flame propagation speed and flame front distance of methane/ethane mixed gas explosion with foam nickel of different porosity. The gray rectangular portion of Fig. 7 indicates flame propagation up to 30 cm (Installation position of nickel foam). It can be seen that the flame velocity only peaks once when the nickel foam successfully quenches the methane/ethane mixture explosion flame. If the flame quenching fails, the propagation process will be accelerated twice, with the first acceleration occurring near 30 cm and the second acceleration occurring near 70 cm to get the second peak velocity. Moreover, the explosive reaction intensifies after flame quenching fails, and the flame may be converted to detonation (DDT) to a certain extent. Hence, the flame propagation rate increases dramatically after the failure of quenching. Fluctuations in the flame propagation speed curve were observed at the pressure relief port at the end of the pipeline. This phenomenon occurs because when the front of the explosion flame reaches the pressure relief port, the flame will be stretched, increasing the speed of flame propagation. When the flame passes through the pressure relief port, the stretching effect weakens, thus forming a similar peak. As shown in Fig. 7, when the quenching effect of foam nickel fails, the flame speed curve fluctuates in the gray area. This is because when the flame passes through foam nickel, it is quenched by the cold wall of porous materials, resulting in the temperature drop of the explosion flame, and the propagation speed also decreases. However, once the flame passes through foam nickel, this cold wall quenching effect will no longer work, rapidly increasing flame speed.

As shown in Fig. 7, when $\phi = 10\%$, because the volume fraction of ethane in the methane/ethane gas mixture accounts for a relatively small percentage, the flame is quenched by 30PPI and 40PPI nickel foam, and no secondary acceleration phenomenon occurs. When $\phi = 20\%$ and the porosity of nickel foam is 30 PPI, a secondary acceleration phenomenon occurs after the flame penetrates the nickel foam, and the peak flame velocity accelerates from 14.88 m/s to 17.06 m/s. When $\phi = 30\%$, similar to Fig. 7(b) when the nickel foam porosity is 30 PPI, the flame also shows a secondary acceleration phenomenon, and the peak velocity of the secondary acceleration is 19.54 m/s. When the nickel foam porosity is 30 PPI, quenching is successful only when the ethane volume fraction is 10%, and quenching fails when the ethane volume fraction is 20% and 30%. The methane/ethane mixture explosion flames is quenched successfully when the nickel foam porosity is 40 PPI. As shown in Fig. 7, in the presence of nickel foam in the explosive pipeline, the explosion propagation velocity increases with the increase of the volume fraction of ethane. Compares Fig. 7 with Fig. 6, the flame propagation velocity is significantly affected when the nickel foam. When quenching is successful, the flame propagation velocity tends to increase and then decrease. When the quench fails, the flame propagation shows two peaks, and the flame speed after passing through the nickel foam is more rapid than the flame speed at the same distance in Fig. 6.

In summary, the analysis shows that nickel foam and volume fraction of ethane affect the velocity of the flame front of the methane/ethane mixture explosion. The addition of ethane increases the flame front speed [22]. Nickel foam promotes or inhibits flame front velocity depending on its porosity. When the nickel foam porosity is 30 PPI, the methane/ethane mixture explosion has two scenarios: quenching successful or quenching failure. When the ethane volume fraction is 10%, quenching successful, the flame front velocity only has one peak, when the ethane volume fraction is 20% and 30%, quenching failure, the flame front velocity only has two peaks, the second peaks is more remarkable compared to the first one. The second acceleration after the flame quenching failure will

promote the flame front, so that the explosion is more violent; when the nickel foam porosity is 40 PPI, the methane/ethane mixture explosion is quenched successfully, and there is only one peak in the flame front velocity, i.e., the flame propagation is accelerated only once.

3.3 Explosion overpressure

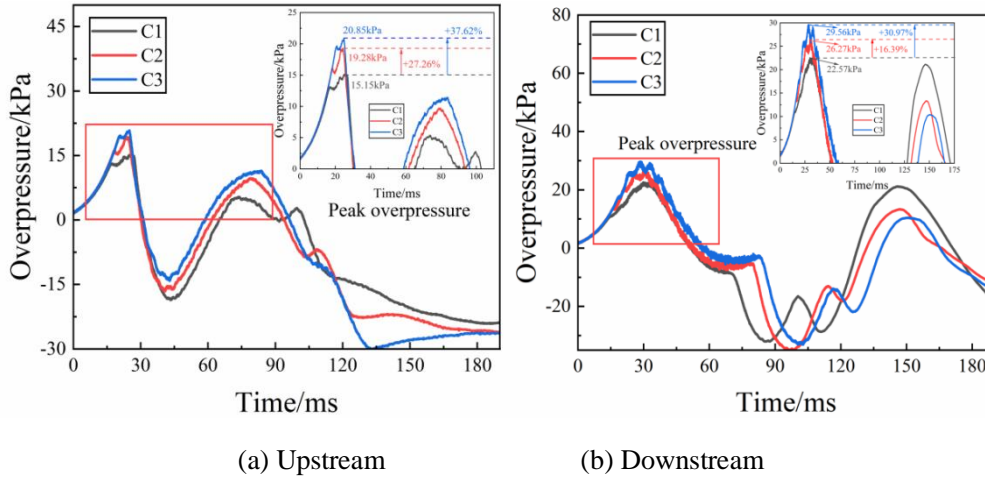
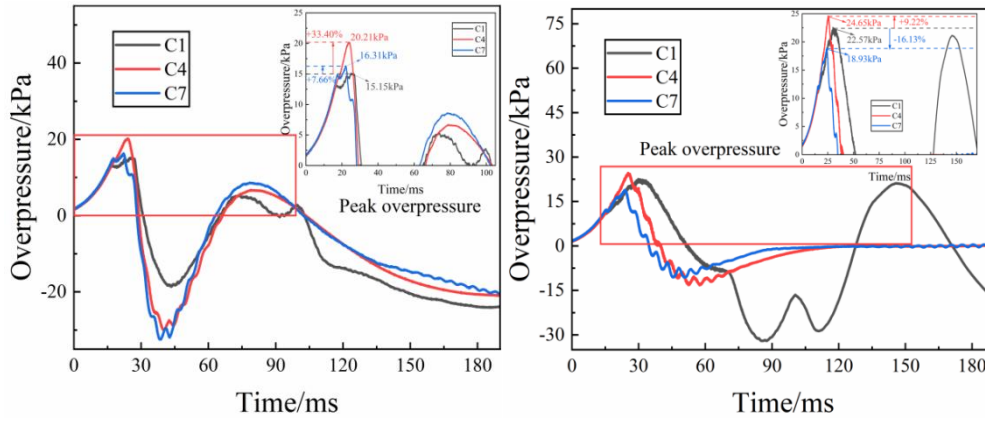


Fig. 8 Dynamic changes of overpressure of methane/ethane mixture explosion in empty pipeline

Fig. 8 shows the dynamic explosion overpressure of methane/ethane explosion in empty pipe, Fig. 8(a) shows the upstream explosion overpressure $P1$, and Fig. 8(b) shows the downstream explosion overpressure $P2$. The figure shows that as the peak explosion overpressure increase with the increase of ethane fraction, indicating that the volume fraction of ethane is positively correlated with the explosion overpressure. In addition, due to the PVC membrane rupture, secondary deflagration, and other factors, the explosion overpressure curve shows multi-peak characteristics. The pressure sensor inside the pipeline records subtle changes during the flame acceleration process. After the overpressure generated by the explosion reached its highest value, significant fluctuations were observed. This phenomenon can be attributed to the reflection of shock waves by the surrounding environment during flame propagation, which propagates in the form of transverse waves in front of the flame, leading to pressure oscillations. Radulescu et al. [23] captured the release of transverse waves inside the pipeline. They compared it with the pressure oscillation data recorded in the experiment, explaining the pressure oscillation inside the pipeline.

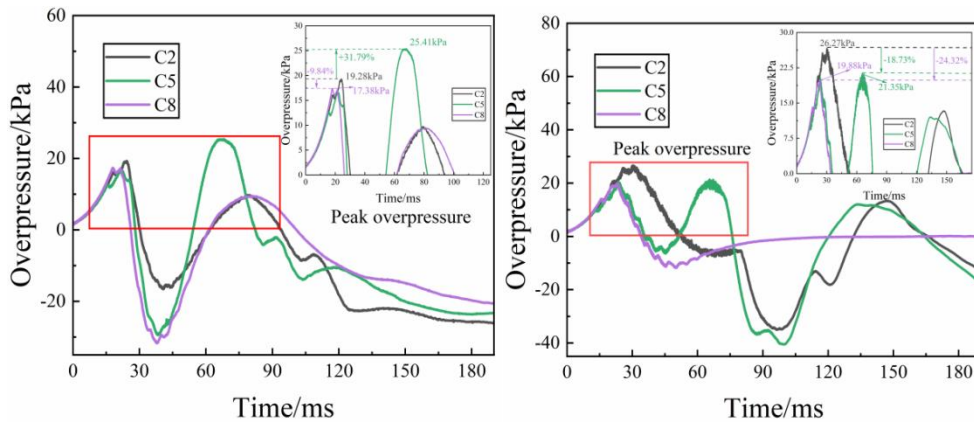
When $\phi = 10\%$, $P1$ peaks at 15.15 kPa and $P2$ peaks at 22.57 kPa; when $\phi = 20\%$, $P1$ peaks at 19.28 kPa and $P2$ peaks at 26.27 kPa, with upstream and downstream increases of 27.26% and 16.39%, respectively, compared to $\phi = 10\%$; when $\phi = 30\%$, $P1$ peaks at 20.85 kPa and $P2$ peaks at 29.56 kPa, an upstream and downstream increase of 37.62% and 30.97%, respectively, compared to $\phi = 10\%$. $P1$ shows a trend of rising, then falling and rising again; the peak of overpressure occurs at about 25ms, and the pressure begins to fall sharply after reaching the peak overpressure, $P2$ rises first and then fall,, its slightly larger compared to $P1$, the peak overpressure time is about 30 ms, and it declines more slowly than $P1$ but with a more pronounced amplitude.



(a) Upstream

(b) Downstream

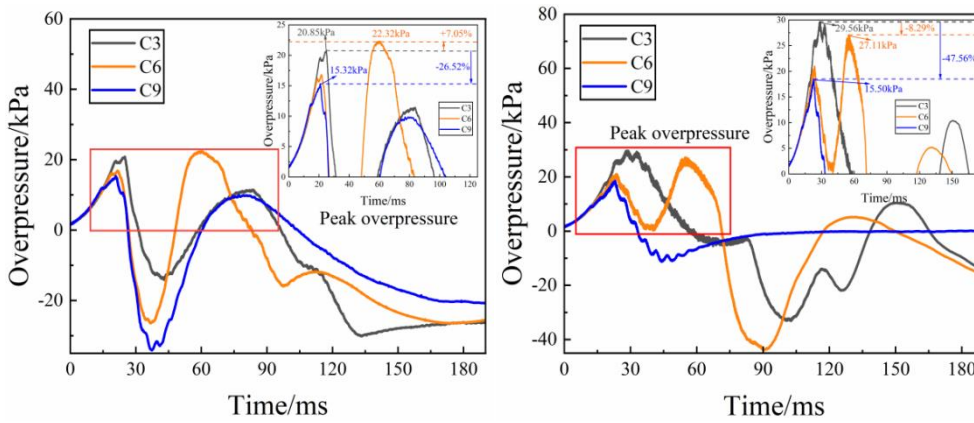
Fig. 9 $\phi=10\%$,effect of foam nickel with different porosity on explosion overpressure of methane/ethane mixture



(a) Upstream

(b) Downstream

Fig. 10 $\phi=20\%$, effect of foam nickel with different porosity on explosion overpressure of methane/ethane mixture



(a) Upstream

(b) Downstream

Fig. 11 $\phi=30\%$,effect of foam nickel with different porosity on explosion overpressure of methane/ethane mixture

[Fig. 9](#), [Fig. 10](#), and [Fig. 11](#) show the effect of nickel foam with different porosity on the explosion overpressure of methane/ethane mixtures while ethane volume fractions $\phi=10\%$, 20% , and 30% , respectively. It can be seen that the effect of nickel foam with different porosity may lead to an increase or decrease in the peak explosion overpressure. In [Fig. 9](#) to [Fig. 11](#), when the nickel foam quenching successfully, the upstream and downstream explosion overpressure change trend is approximately the same. There is only one peak value of upstream and downstream overpressure. When flame quenching failure, the explosive reaction intensifies, and the downstream peak overpressure is larger than the upstream. This indicates that the failure of flame quenching will increase the explosion overpressure; the reason is that the nickel foam fails to block the flame; its solid-phase structure acts as an obstacle, so the flame burns more vigorously, and the explosion overpressure is also increased. The phenomenon of wave peaks accompanied by fluctuations in the overpressure graph is due to the repeated vibration of the pressure curve, resulting in the formation of multiple peaks. This phenomenon is mainly due to the membrane rupture during the propagation of the explosion shock wave, resulting in a significant decrease in the overpressure generated by the explosion. After pressure relief, the explosion overpressure exhibits oscillatory characteristics with enhanced turbulence intensity due to the increase of vortices. The first observation in the overpressure image is that the maximum overpressure peak of the premixed gas downstream in the pipeline is maintained for a longer period compared to the maximum upstream pressure, and this peak is determined by the competition between multiple peaks [24].

As shown in [Fig. 9](#), when the volume fraction of ethane is 10% , the upstream peak overpressure increases by 33.40% and 7.66% with the increases of the porosity of nickel foam, respectively; the downstream peak overpressure of 30 PPI nickel foam decreases by 16.13% , and the downstream peak overpressure of 40 PPI nickel foam increases by 9.22% . As shown in [Fig. 10](#), when the volume fraction of ethane is 20% , compared with the empty tube, the upstream peak overpressure of 30 PPI nickel foam increases by 31.79% , and the upstream peak overpressure of 40 PPI nickel foam decreases by 9.84% ; with the increase in the porosity of nickel foam, the downstream peak overpressure decreases by 18.73% and 24.32% , respectively. As can be seen in [Fig. 11](#), when the volume fraction of ethane is 30% , compared with the empty pipe, the upstream peak overpressure of 30 PPI nickel foam increases by 7.05% , the upstream peak overpressure of 40 PPI nickel foam decreases by 26.52% ; with the increase in the porosity of the nickel foam, the downstream peak overpressure decreases by 8.29% and 47.56% , respectively.

In summary, it can be concluded that the explosion overpressure is affected by the ethane volume fraction. Nickel foam's promotion or suppression depends on its porosity. When the flame is quenched, the porous material can effectively suppress the explosion overpressure and the suppression effect is weakened with the increase of the ethane volume fraction; when the flame quenching failure, the downstream explosion overpressure increases abruptly, and the upward tendency is strengthened with the increase of the ethane volume fraction.

3.4 Mechanism analysis

In this paper, the porous material is placed vertically in an explosion experimental pipe, and the primary investigation is focus on the quenching behavior of porous materials on flames [26]. According to the cold wall quenching mechanism of porous materials, when the flame is in contact with the porous material, its particular pore structure can shear and split the flame, resulting in multiple collisions between the flame and the internal pore structure of the porous increases the contact area with the pore wall, the porous material reduces the flame's temperature through heat transfer and energy absorption until it reaches the quenching temperature to extinguish the flame [27]. The pore structure of porous materials leads to an increase in the concentration of upstream premixed gases, which increases the frequency of free radicals colliding with the pore walls and reduces the number of free radicals effectively involved in the combustion reaction, which in turn inhibits the formation and propagation of flames [28]. In addition, the porous medium has a suppression effect on the blast shock wave. When the shock wave contacts the porous material, part of the energy of the shock wave will be dissipated by the reflection of the solid surface; the irregular pores inside the porous material will lead to the reflection and scattering of the shock wave, forming a reflected pressure wave, which further dissipates the energy [29]. These reflected pressure waves interfere with flame propagation, causing the flame structure to become dispersed and reducing the flame propagation velocity.

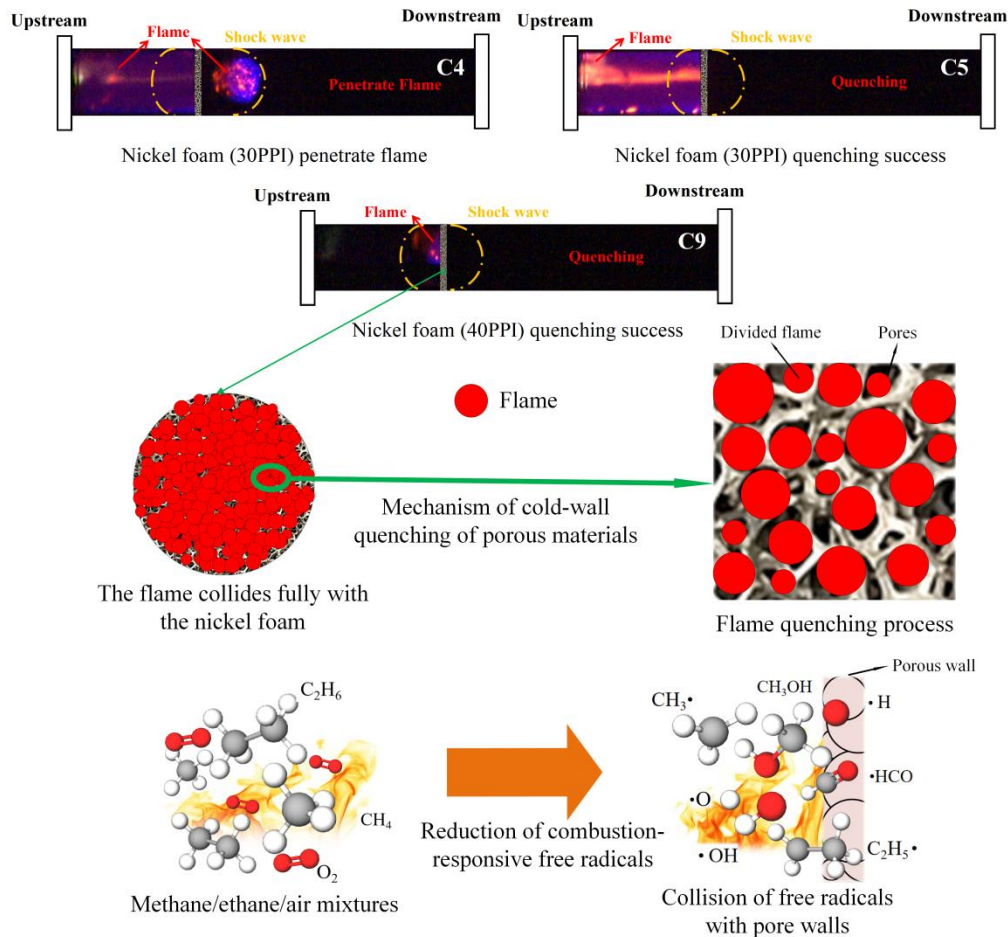


Fig. 12 Mechanism of porous material effect on explosion flame propagation

Combining the quenching and pressure decay mechanisms of porous materials mentioned above, the mechanism of nickel foam on the flame propagation of methane/ethane mixture explosion is explored. As can be seen from Fig. 12, when the nickel foam porosity is 30PPI, the explosion flame has the effect of both promoting and inhibiting, this is because the explosion intensity is related to the volume fraction of ethane in the gas mixture, the flame propagation speed and explosion overpressure with the volume fraction of ethane is proportional. When the explosion flame quenching fails, nickel foam as an obstacle to accelerate the flame spread, and the flame breaks through the porous nickel foam bondage ignited downstream gas, causing the secondary deflagration phenomenon; when the explosion flame quenching success, the flame can not penetrate the nickel foam, nickel foam inhibits the flame propagation successfully. When the nickel foam porosity is 40PPI, with the increase of nickel foam porosity, the nickel foam cold wall quenching effect is enhanced, and also the free radicals collision of the pore wall, which reduces the number of free radicals that are effectively involved in the combustion reaction, and inhibits the formation and propagation of the flame.

Therefore, it can be concluded that nickel foam may have two different effects on the flame propagation of methane/ethane mixture explosion: quenching successful and quenching failure. Quenching failure will accelerate the flame propagation so that the explosion intensifies; nickel foam porosity of 30ppi explosion suppression is limited; nickel foam porosity of 40ppi explosion suppression effect is significant, the explosion flame quenching successful. Larger porosity provides better safety protection for methane/ethane gas explosions.

4 Conclusion

This paper investigates the technology of nickel foam to suppress the explosion of methane/ethane mixtures and analyzes the explosion characteristics of methane/air-premixed gases. The main results are summarized as follows:

(1) Nickel foam has two effects on the methane/ethane mixture: explosion flame promotion and inhibition. When quenching failure, the peak velocity and peak overpressure appears in the second peak; When quenching successfully, the flame propagation is blocked, and the peak flame velocity and overpressure decreases, and the peak value of velocity and pressure appears in the first wave peak.

(2) Flame velocity and explosion overpressure changes is affected by ethane volume fraction. When the flame is quenched, the porous material can effectively inhibit the explosion overpressure and flame propagation speed. The inhibition effect weakened with the increase of ethane volume fraction. When the flame quenching fails, the explosion overpressure and flame propagation velocity increases abruptly.

(3) The porosity of porous materials has a significant impact on explosions. When the porosity is low, it may result in successful or failed explosion suppression. The probability of suppression successful increases with the increases of porosity of porous materials , larger porosity provides greater safety assurance.

Acknowledgment

This work was supported by the Science and Technology Research Program of Chongqing Municipal Education Commission (KJZD-K202401501); National Natural Science Foundation of China (52274177). Thanks.

References

- [1] Sun, S, et al., Effects of concentration and initial turbulence on the vented explosion characteristics of methane-air mixtures, *Fuel*, 267 (2020): 117103.
- [2] Erjiang, H, et al., Experimental Study on Ethane Ignition Delay Times and Evaluation of Chemical Kinetic Models. (2015).
- [3] Golovastov, S V., et al., Evolution of detonation wave and parameters of its attenuation when passing along a porous coating, *Experimental Thermal and Fluid Science*, 100 (2019): 124-134.
- [4] Su, B, et al., Coupling analysis of the flame emission spectra and explosion characteristics of CH₄/C₂H₆/air mixtures, *Energy & Fuels*, 34.1 (2019): 920-928.
- [5] Luo, Z, et al., Experimental study on the deflagration characteristics of methane-ethane mixtures in a closed duct, *Fuel*, 259 (2020): 116295.
- [6] Duan, Y, et al., Experimental study on methane explosion characteristics with different types of porous media, *Journal of Loss Prevention in the Process Industries*, 69 (2021): 104370.
- [7] Cao, X, et al., Experimental research on the characteristics of methane/air explosion affected by ultrafine water mist, *Journal of hazardous materials*, 324 (2017): 489-497.
- [8] Wang, L, et al., Synergistic suppression effects of flame retardant, porous minerals and nitrogen on premixed methane/air explosion, *Journal of Loss Prevention in the Process Industries*, 67 (2020): 104263.
- [9] Yang, W, et al., Effect of ignition position and inert gas on hydrogen/air explosions, *International journal of hydrogen energy*, 46.12 (2021): 8820-8833.
- [10] Jianhua, S, et al., The comparative experimental study of the porous materials suppressing the gas explosion, *Procedia Engineering*, 26 (2011): 954-960.
- [11] Duan, Y, et al., Exploration of critical hydrogen-mixing ratio of quenching methane/hydrogen mixture deflagration under effect of porous materials in barrier tube, *International Journal of Hydrogen Energy*, 48.58 (2023): 22288-22301.
- [12] Cui, Y. Y., et al., Effect of wire mesh on double-suppression of CH₄/air mixture explosions in a spherical vessel connected to pipelines, *Journal of Loss Prevention in the Process Industries*, 45

- (2017): 69-77.
- [13] Nie, B, et al., The roles of foam ceramics in suppression of gas explosion overpressure and quenching of flame propagation, *Journal of Hazardous Materials*, 192.2 (2011): 741-747.
- [14] Pang, L, et al., A study on the characteristics of the deflagration of hydrogen-air mixture under the effect of a mesh aluminum alloy, *Journal of Hazardous Materials*, 299 (2015): 174-180.
- [15] Yulong, D, et al., Characteristics of gas explosion to diffusion combustion under porous materials, *Explosion and Shock Waves*, 40.9 (2020): 095401-1.
- [16] Long, F, et al., Effect of porous materials on explosion characteristics of low ratio hydrogen/methane mixture in barrier tube, *Journal of Loss Prevention in the Process Industries*, 80 (2022): 104875.
- [17] Wu, S., Experimental Study on the Suppression of Explosion Flame in Pipelines with Porous Materials, Chongqing University of Science and Technology, Chongqing, China, 2018
- [18] Zhou, S, et al., Effects of mesh aluminium alloy and aluminium velvet on the explosion of H₂/air, CH₄/air and C₂H₂/air mixtures, *International Journal of Hydrogen Energy*, 46.27 (2021): 14871-14880.
- [19] Pei, B, et al., Experimental study on the synergistic inhibition effect of nitrogen and ultrafine water mist on gas explosion in a vented duct, *Journal of Loss Prevention in the Process Industries*, 40 (2016): 546-553.
- [20] Ibrahim, S. S., and A. R. Masri., The effects of obstructions on overpressure resulting from premixed flame deflagration, *Journal of Loss Prevention in the Process Industries*, 14.3 (2001): 213-221.
- [21] Hu, E, et al., Experimental and numerical study on the effect of composition on laminar burning velocities of H₂/CO/N₂/CO₂/air mixtures, *international journal of hydrogen energy*, 37.23 (2012): 18509-18519.
- [22] Luo, Z, et al., Experimental study on the deflagration characteristics of methane-ethane mixtures in a closed duct, *Fuel*, 259 (2020): 116295.
- [23] Radulescu M I, Lee J H S. The failure mechanism of gaseous detonations: experiments in porous wall tubes. *Combustion & Flame*, 131(1/2) (2002):29-46.
- [24] Ma Q, et al. Effects of hydrogen addition on the confined and vented explosion behavior of methane in air. *Journal of Loss Prevention in the Process Industries*, 27 (2014): 65-73.
- [25] Rocourt X, et al. Vented hydrogen–air deflagration in a small enclosed volume. *International Journal of Hydrogen Energy*, 39(35) (2014): 20462-20466.
- [26] Heinrich, A, et al., Investigation of the turbulent near wall flame behavior for a sidewall quenching burner by means of a large eddy simulation and tabulated chemistry, *Fluids*, 3.3 (2018): 65.
- [27] Wang, M, et al., Effect of metal foam mesh on flame propagation of biomass-derived gas in a half-open duct, *ACS omega*, 5.32 (2020): 20643-20652.
- [28] Wang, L, et al., Synergistic suppression effects of flame retardant, porous minerals and nitrogen on premixed methane/air explosion, *Journal of Loss Prevention in the Process Industries*, 67 (2020): 104263.
- [29] Chen, P, et al., Effects of metal foam meshes on premixed methane-air flame propagation in the closed duct, *Journal of loss prevention in the process industries*, 47 (2017): 22-28.

Submitted: 07.09.2024.
Revised: 18.10.2024.
Accepted: 20.10.2024.